www.arpnjournals.com

SIMULATION OF AIR RESIDENCE TIME DISTRIBUTIONS OF SPRAY DROPLETS IN A COUNTER-CURRENT SPRAY DRYER

Eyitayo A. Afolabi and K. R. Onifade
Department of Chemical Engineering, Federal University of Technology, Minna, Nigeria
E-Mail: elizamos2001@yahoo.com

ABSTRACT

This research focused on the development of a fundamental model that can be used to predict the air residence time distribution of spray droplets in a counter-current spray dryer. The proposed model consists of two parallel sections. Firstly, two continuous stirred tanks and a plug-flow in between and secondly, a plug-flow and a stirred tank. A FORTRAN 77 program using Runge Kutta-Mersion subroutine was used to simulate the three first order differential and two linear model equations. The simulated results showed that at high water and airflow rates, more droplets enter into the mixing zones and large amount of moisture content evaporated at a short time interval. There was good agreement between the experimental data and simulated results airflow patterns which make it suitable for industrial application and the standard deviations obtained are within the acceptable limit.

Keywords: residence time distribution, spray droplet, spray dryer, air flow pattern.

1. INTRODUCTION

Intensive research and development during the last two decades have showed that spray drying is a highly competitive means of drying a wide variety of products. Spray drying is a well-established method for converting liquid or slurry feed materials into a dry powder form (Masters, 1991). It is widely used to produce powdered food, healthcare and pharmaceutical products. Often, spray drying comes at the end-point of the processing line, as it is an important step to control the final product quality. Spray drying has the great advantage that products can be dried without much loss of volatile or thermal liable compounds. Others include rapid drying rates, a wide range of operating temperatures and short residence times. In everyday application, spray drying process cut across all major industries ranging from production in the most delicate of condition laid down in food and pharmaceutical manufacture, right through the high - tonnage outputs within such heavy chemical fields as mineral ores and clays (Masters, 1991).

As shown in Figure-1, spray drying consists of four stages of operation: (1) atomization of liquid feed into a spray chamber; (2) contact between the spray and the drying medium; (3) moisture evaporation; and (4) separation of dried products from air stream. Each stage is carried out according to dryer design and operation, together with the physical and chemical properties of the feed; this determines the characteristics of the dried products. In the counter-current spray dryer configuration, the feed materials and drying medium enter at the opposite ends of the drying chamber. Here, the outlet product temperature is higher than the exhaust air temperature, and is almost at the feed-air temperature with which it is in contact. This arrangement offers dryer performance with excellent heat utilization and mostly used for drying non heat sensitive products. However, it does subject the driest powder to the hottest air stream (Kuriakose and Anandharamakrishnan, 2010; Qakley, 2004).
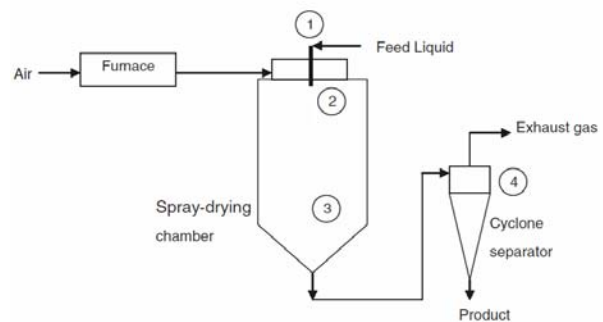
Figure-1. Stages of operation in a spray dryer (Kuriakose and Anandharamakrishnan, 2010).

The time it takes a molecule to pass through a reactor is called residence time, Θ. Two properties of Θ are important. The time elapsed since the molecule entered the reactor (its usage) and the remaining time it will spend in the reactor (its residual lifetime). A convenient definition of residence-time distribution function is the function J (Θ) of the effluent stream that has a residence time less than Θ. The residence time distribution for a given reactor and flow rate can be established from response type's experiments. In these experiments the concentration of an inert tracer is perturbed in the feed stream and its effect on the effluent stream is measured; the three most common perturbations are a step function, a pulse (square wave) and a sinusoidal wave (Luyben, 1996). The particle residence time has a great impact on the final powder qualities, such as solubility and bulk density. The residence time profile is basically divided into two parts; namely, primary and secondary residence times. The primary residence time is calculated from the time taken for droplets leaving the nozzle to impact on the wall or leave at the outlet. The secondary residence time can be defined as the time taken for a particle to slide along the wall from the impact position to the exit (Kuriakose and Anandharamakrishnan, 2010). "The jet or

nozzle zone" and the "free entrainment zone" are the zones commonly observed by researchers who studied the flow pattern of spray droplets in a spray dryer. Gauvin *et al*. (1977) and Katta *et al*. (1976) used this conclusion to predict the droplet trajectory for water spray and found good agreement with experimental results. Ade-John and Jeffreys, (1973), Onifade, (1983) used iodine solution in potassium iodide as tracer to visualize flow and obtain residence time distribution of water and slurry in spray dryer. They found that the drop phase residence time increased with higher airflow rates. However, much more detailed analysis of the result was hindered due to their inability to eliminate the delay imposed by the accumulation of the tracer on the wall of the dryer. Kieviet (1997) and Kieviet *et al*. (1997) investigated what particles experience in the drying chamber with respect to air temperature and humidity. They measured and modelled the particle trajectories and product residence time distributions using hot wire anemometer and CFD respectively. The modelled airflow pattern proved to consist of a fast flowing core and a slow circulation around the core. This agreed well with experimental observations.

The use of dispersion models to describe the flows in reactors such as packed beds and packed columns was extended to characterize the air flow patterns in terms of a mixture of "plug flow" zone, "well-stirred tank" zone and "air inert" zone caused the by-pass stream. A flow model consisting of two stirred tanks in parallel with a plug by-pass is one of many models proposed to study spray in counter current arrangement (Fletcher and Langrish, 2003; Menshutina and Kudra, 2001). The model mirrored a rapidly ascending central core surrounded by annular zone of intense turbulence. Ade-John and Jeffreys (1973), Onifade (1983) proposed a model consisting of two well stirred tanks separated by a plug flow zone, the three in parallel with a by-pass stream to describe the flow characteristics of air in a counter-current spray dryer. The aim of the present study is to develop model equations representing the air residence time distribution of spray droplets in a counter current spraying dryer. These model equations are then simulated and the simulated results compared with experimental data.

2. METHODOLOGY

2.1. The proposed droplets' residence time distribution model

The model used in this work is an extension of those used by Ade-John and Jeffreys (1978) and Onifade (1983) for predicting the residence time distribution of air in a counter spray dryer. These models were based on a visual observation of the flow patterns of smoke injected into the air-stream from which different zones are identified. As shown in Figure-1, the present model is made up of two sections; the first consists of two stirred tank separated by a plug-flow. The second consists of a plug flow and a stirred tank.
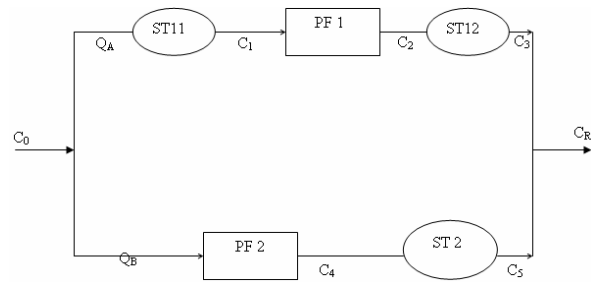
Figure-2. Proposed diagrammatic model array for droplets residence time distribution.

Development of model equations

In analysis residence time distribution (RTD) data, gamma function is particularly useful if the volume of the zones can be determined accurately. For example, the smoke experiment was used by Ade-John and Jeffreys, (1973) to determine RTD of air flow in a counter-current spray dryer. In the absence of such a determination, the overall equations that evolve from Gamma counter function analysis are in form of non-linear equations with six parameters. These equations required rigorous and tedious regression, which is best, handled by powerful non-linear regression packages or by other optimisation techniques (Menshutina and Kudra, 2001). The present work resort to the use of first order reaction equations (Ameh, 2003; Afolabi, 2004).

With respect to Figure-2, the following notations are used.

(a)

ST11	1st stirred tank in section 1	Volume	V_1
ST12	2nd stirred tank in section 1	Volume	V_k
ST2	Stirred tank in section 2	Volume	V_N
PF1	Plug-flow in section 1	Volume	V_J
PF2	Plug-flow in section 2	Volume	V_M

(b) A, B - the ratio of the flow of the injected tracer particle into section 1 and 2, respectively.

(c)
J   fraction by volume of PF1
K   fraction by volume of ST12
M   fraction by volume of PF2
N   fraction by volume of ST2

(d) Q_A, Q_B - the flow rates into section 1 and 2, respectively

(e) Q_T, V_T - the total flow rate and volume in the two sections, respectively.

$$A = \frac{Q_A}{Q_T} \tag{1}$$

$$B = \frac{Q_B}{Q_T} \tag{2}$$

From (a), (c) and (e)

www.arpnjournals.com

$$K = \frac{V_K}{V_T} \tag{3}$$

$$N = \frac{V_N}{V_T} \tag{4}$$

$$J = \frac{V_J}{V_T} \tag{5}$$

$$M = \frac{V_M}{V_T} \tag{6}$$

The fraction by volume in ST 11 $=$ 1 - J –K-M-N

$$\frac{V_1}{V_T} = \text{ 1 - J –K-M-N} \tag{7}$$

ST 11 Region

$$V_1 \frac{dC_1}{dt} = Q_A(C_0 - C_1) \tag{8}$$

$$\frac{dC_1}{dt} = \frac{Q_A}{V_1}(C_0 - C_1)$$

From (1), $Q_A = Q_T A$ and equation (7) gives

$$V_1 = \text{ 1 - J –K-M-N}$$

Then, on substitution into equation (8)

$$\frac{Q_A}{V_1} = \frac{AQ_T}{(1 - J - K - M - N)} \tag{9}$$

$$= \frac{Q_A}{V_1}$$

But $t = \frac{Q_A}{V_1}$ on substitution, equation (9) becomes

$$\frac{Q_A}{V_1} = \frac{A}{(1 - J - K - M - N)} \tag{10}$$

Put (10) into (8)

$$\frac{dC_1}{dt} = \frac{A(C_0 - C_1)}{t(1 - J - K - M - N)} \tag{11}$$

In dimensionless form

$$\theta = \frac{t}{\bar{t}}$$

Therefore, $dt = \overline{td\theta}$ \tag{12}

$$\frac{dC_1}{dt} = \frac{A(C_0 - C_1)}{(1 - J - K - M - N)} \tag{13}$$

PF 1 Region
This region constitutes a time delay and the only requirement for simulation exercise is to calculate the time delay θ_J

$$T_J = \frac{V_J}{Q_A} \tag{14}$$

From equations (1) and (5), equation (14) becomes

$$T_J = \frac{TV_T}{AQ_T} \tag{15}$$

$$= \frac{V_T}{Q_T}$$

Since t

$$T_J = \frac{Jt}{A}$$

$$\frac{T_J}{t} = \frac{J}{A}$$

$$\theta_J = \frac{J}{A} \tag{16}$$

ST 12 Region

$$\frac{dC_3}{dt} = \frac{Q_A}{V_K}(C_2 - C_3) \tag{17}$$

Using (1) and (3), performing the same substitution as for ST 11 gives

$$\frac{dC_3}{d\theta} = \frac{A}{K}(C_2 - C_3) \tag{18}$$

PF 2 Region

Time delay is only required,

$$T_m = \frac{V_m}{Q_B} \tag{19}$$

From equations (2) and (6), using the same procedure as for PF 1, equation (19) gives

$$\theta_J = \frac{M}{B} \tag{20}$$

ST 12 Region

$$\frac{dC_5}{dt} = \frac{Q_B}{V_N}(C_4 - C_5) \tag{21}$$

Using (2) and (4), performing the same substitution as for ST 11 equation (21) gives

$$\frac{dC_5}{d\theta} = \frac{B}{N}(C_4 - C_5) \tag{22}$$

The total response from the simulation is the summation of the concentration from the two sections and is given by

$$C_R = C_3 + C_5 \qquad (23)$$

2.2. Simulation programme

The exit concentration profile of the tracer for a particular water flow rate was used as the inlet experimental data (pulse) and constitutes the C_o, while the exit concentration profiles of the tracer in that water flow rate for various air flow rates constitutes the experimental response data (Onifade, 1983). Runge Kutta Mersion routine was used to solve the first order equations and the whole simulation exercise was carried out using a WATFOR 3.0 FORTRAN program. Values of A, B, J, K, M, N were varied until a close fitting occurred between the overall exit response (C_R) obtained from simulation and experimental response data. Experimental data for five different air flow rates against one water flow rate for WMF nozzle and another five set for SDX nozzle were selected from the work of Onifade, (1983) to validate the model equations developed. The experimental measurements obtained were in the form of pulse and response data. However, the real time components of the data were later converted into dimensionless form.

3. RESULTS AND DISCUSSIONS

The parameters obtained from the various zones and streams of the model, the standard deviation between the experimental and model response data are summarized in Tables 1 and 2. Comparison of the experimental data and simulated results are shown in Figures 3 and 4.

Table-1. Parameters and standard deviation for WMF nozzles.

	A	B	J	K	M	N	Standard deviation
WMF 2	0.750	0.250	0.120	0.101	0.008	0.004	5.8313
WMF 3	0.650	0.350	0.130	0.014	0.007	0.005	3.0930
WMF 4	0.750	0.250	0.100	0.014	0.008	0.006	3.2226
WMF 5	0.850	0.150	0.100	0.010	0.005	0.005	4.2493
WMF 6	0.900	0.100	0.100	0.008	0.004	0.003	4.0344

Table-2. Parameters and standard deviation for SDX nozzles.

	A	B	J	K	M	N	Standard deviation
SDX 20	0.778	0.222	0.080	0.050	0.009	0.005	4.2937
SDX 21	0.750	0.250	0.150	0.080	0.007	0.003	3.2174
SDX 22	0.740	0.260	0.150	0.090	0.009	0.003	3.3676
SDX 23	0.745	0.255	0.100	0.010	0.007	0.002	3.9612
SDX 24	0.720	0.280	0.100	0.070	0.008	0.003	5.3865

www.arpnjournals.com
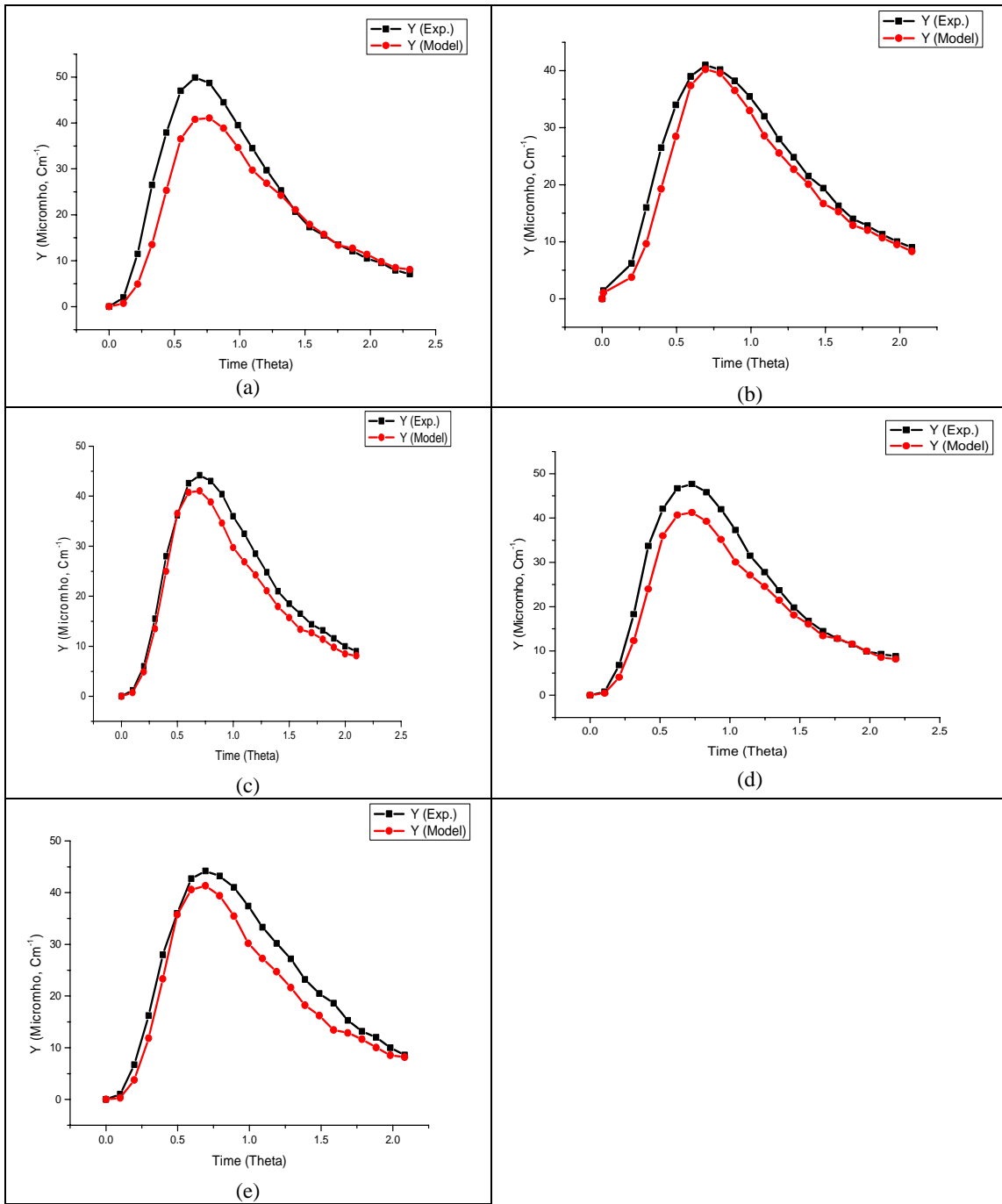
Figure-3. Variation of concentration with time for: (a) WMF 2 (b) WMF 3 (c) WMF 4 (d) WMF 5 (e) WMF 6.

www.arpnjournals.com
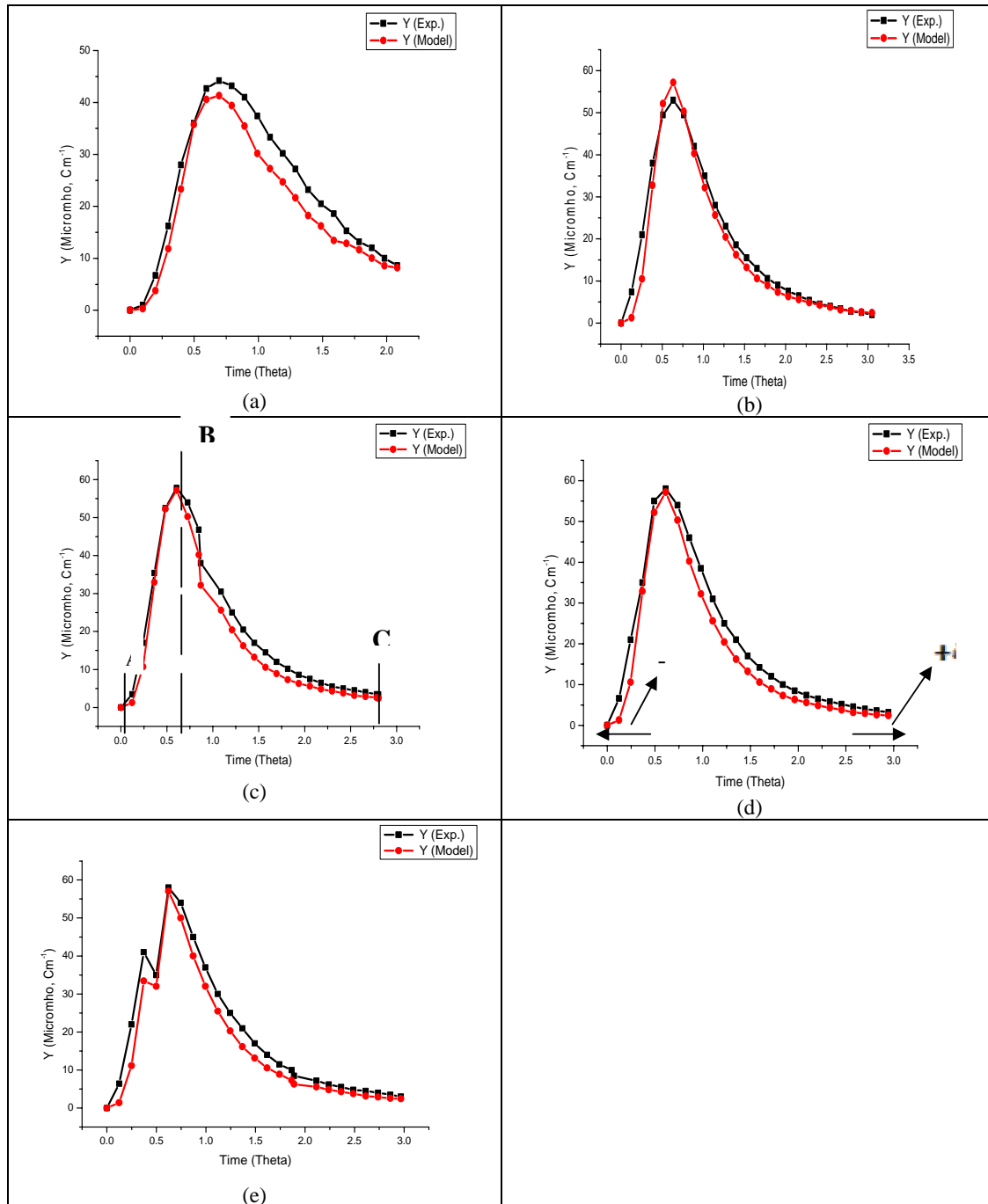
Figure-4. Variation of concentration with time for: (a) SDX 20 (b) SDX 21 (c) SDX 22 (d) SDX 23 (e) SDX 24.

3.1. Discussions of results

Tables 1 and 2 show that the fraction of A is greater than that of B, meaning majority of the droplets reside mainly in stream A. For example, Table-1 shows an initial drop in the value of airflow rate for parameter A from 0.750 to 0.650 and subsequently, a rise from 0.750 to 0.800 and finally to 0.900. Most of the droplets residing in stream A proved that, as air flow rate increases from WMF 2 to WMF 6, more of the flow goes into the section

containing more mixing zones, ST11 and ST12. In addition, the sum of the fractions K, N and (I-J-K-M-N) of the mixing zones ST11, ST12 and ST2 increases from WMF 2 to WMF6. That is, as air flow increases, mixing are intensified in the continuous stirred tank zones. This increase in the airflow rates resulted in the spray cloud becoming denser with droplets that spread outwards into the mixing zones. Therefore, a large amount of the moisture content is evaporated within a very short-time

interval. As shown in Table-2 the same pattern is observed for SDX nozzles. However, unlike in Table-1, the trend in the values of A in Table-2 is erratic. It decreases from the first row to the third, increases in the fourth and decreases in the fifth. This is accompanied by a corresponding increase, decrease and increase in B. Incidentally, when the value of B increases as in the first row to the third, the proportion going into the plug-flow zones also increases, showing that less drop enter the "active" mixing zones.

There is mutual agreement between the simulation results and experimental data as shown in Figures 3 and 4. This is based on the closeness of the movement of the graphs to each other. Figures 3 and 4 illustrate that the drying process is not smooth but a continuous one. For example, point AB in Figure-4(c) represents a condition where the surface is capable of supplying sufficient free moisture to saturate the air in contact with it and is often referred to as the first period of drying. However, point BC represents the second period of drying where the entire drying process occurred in the falling-rate period. In this region, the initial moisture content is found to be less than the critical moisture content. That is, the surface is no longer capable of supplying sufficient free moisture to saturate the air in contact with it. Therefore, the rate of drying depends very much on the mechanism of diffusion by which the moisture from inside the material is transferred to the surface.

In the first period of drying, a large amount of moisture is observed to be evaporated at a very short interval. However, more time is required to evaporate water at low moisture content during the second period of drying. For example, the peak of the curve in Figure-4(c) occurred at $\theta = 0.613$ and concentration = 58 micromho and decreased to a concentration of 3.20 micromho at $\theta=2.945$. The trend observed in Figure-4(c) is the same for the remaining graph and is quite similar to those profiles observed in the works of Ade-John and Jeffreys (1973), Onifade (1983) and Ameh (2002).

The critical and most acceptable interpretation of a standard deviation is in terms of the percentage of cases included within the range of one standard deviation below the mean to another standard deviation above the mean (Guilford and Frutcher, 1987). In a normal distribution, the range from -1 δ to +1 δ must not contain more than 68.23% of the cases. Figure-4(d) illustrates the division of the area under the normal curve into regions marked off at -1 δ to +1 δ. This example yields up to 17 cases and translates to 68% of the total occurrence.

Guilford and Frutcher (1987) found that the standard deviation for the total range of measurements with N equals 20 to 40 must not exceed the range of 3.1 to 4.3. Majority of the calculated standard deviations as shown in Tables 1 and 2 falls within this acceptable range. This shows that the simulated profile is very close to the experimental data. For example, the standard deviation of 4.0344 for WMF 6 multiplies by 3.7 (average of the given range of 3.1 to 4.3) gives an expected range of about 15 cases. This translated to a 68.18% of the whole region.

4. CONCLUSIONS

The results showed that at high water and airflow rates, more droplets enter the mixing zones: ST11, ST12 and ST2. Stream A was observed to contain more water droplets. Analysis of the simulation results show that at high water and air flow rates, greater mixing of spray and air occurred thereby enabling coarser sprays to be dried per given chamber size at a short time interval. The simulation results confirmed that majority of spray evaporation is completed within a short-time interval. This means, the mean size of the pure liquid spray increases with time due to the rapid completion of evaporation of the smaller droplet sizes in the spray. The statistical analysis confirmed that there is a close agreement between the simulated result and experimental data, as the standard deviation obtained are within the acceptable limit.

REFERENCES

Ade-John A. O. and Jeffreys G. Y. 1978. Flow Visualization and Residence Time Studies in a Spray Drier. Trans Ichem, E. 56(1): 36-42.

Afolabi E.A. 2004. Study of Residence time distributions of Spray droplets in a counter current spray dryer, M. Eng. Thesis, Federal University of Technology, Minna, Nigeria.

Ameh Kenneth. 2003. Modelling and Simulation of Air Residence Time Distribution in Spray Dryers. Postgraduate Diploma Thesis, Federal University of Technology, Minna, Niger State. pp. 15-16.

Fletcher D and Langrish T. 2003. Prospects for modelling and design of spray driers in the 21st century. Drying Technology. 21: 197-215.

Gauvin W. H., Bank N. and Reiklin F. A. 1977. Measurements of Flow Characteristics in a Confined Vortex Flow. Canada Journal of Chemical Engineers. 55: 397-402.

Guilford J. P. and Fruchter B. 1987. Fundamental Statistics in Psychology and Education. 6th Edition, McGraw-Hill Book Company. pp. 68-70.

Katta S., Crosby E. J. and Gauvin W. H. 1972. Basic Concepts of Spray Drying Design. Aiche Journal. 22: 665-672.

Kieviet F. G., Van Raaij J. and De Moor P.J.A.M. 1997. Air Temperatures and Humidities in a Co-Current Pilot Spray Dryer. Measurements and Modelling Trans Ichem E. pp. 8-15.

Kieviet F. G. 1997. Modelling Quality in Spray Drying, Ph. D Thesis, Eindhoven University of Technology, the Netherlands. pp. 3-15, 70-89.

www.arpnjournals.com

Kuriakose Rinil and Anandharamakrishnan C. 2010. Computational fluid dynamics (CFD) applications in spray drying of food products. Trends in Food Science and Technology. 21(8): 383-398.

Luyben L. W. 1996. Process Modelling, Simulation and Control for Chemical Engineering. 3rd Edition, McGraw Hill International. pp. 219-221, 93-94, 121-123.

Masters K. 1991. Spray Drying Handbook, 6th Edition, Longman Scientific and Technical Essex. pp. 1-45, 145-167.

Menshutina N.V and Kudra T. 2001. Computer aided drying technologies. Drying Technology. 19(8): 1825-1849.

Onifade K.R. 1983. Studies of Droplet Behaviour in Spray Drying Towers. Ph. D Thesis, University Of Aston, Birmingham, United Kingdom. pp. 64-68, 71, 74, 78, 117 and 119.

Oakley D. E. 2004. Spray dryer modeling in theory and practice. Drying Technology. 22(6): 1371-1402.